Quantifying mass transfer in permeable media containing conductive dendritic networks

Steven M. Gorelick,[1] Gaisheng Liu,[2] and Chunmiao Zheng[2]

Received 15 May 2005; revised 25 July 2005; accepted 17 August 2005; published 20 September 2005.

[1] Tree-like branching networks are conduits for mass transport in many natural systems. Because precisely determining conduit-matrix mass transfer requires exact knowledge of dendrite geometries, interdomain mass exchange rates are often described using the concept of effective mass-transfer. We present a direct association between average geometric properties of dendritic networks and mass transfer. We show that the value of the mass-transfer rate coefficient can be estimated directly using a physically based relation that requires no knowledge of the specific network geometry. **Citation:** Gorelick, S. M., G. Liu, and C. Zheng (2005), Quantifying mass transfer in permeable media containing conductive dendritic networks, *Geophys. Res. Lett.*, *32*, L18402, doi:10.1029/2005GL023512.

1. Introduction

[2] Conductive pathways are often surrounded by relatively homogeneous, lower permeability regions in plant venation [*Roth-Nebelsick et al.*, 2001; *West et al.*, 1999; *Enquist*, 2002], animal vascular [*Beard and Bassingthwaighte*, 2000a; *Nagao et al.*, 2001; *Barber et al.*, 2003; *Beard et al.*, 2003], and natural water-bearing porous media [*Florea and Wicks*, 2001; *Clemens et al.*, 1999] systems. Solute exchange between the two domains is a mass-transfer process. Solutes flowing through conductive conduits and comparatively immobile solutes residing in the surrounding matrix migrate between the two domains by molecular diffusion or slow advection [*Feehley et al.*, 2000; *Harvey and Gorelick*, 2000; *Mustafa et al.*, 1999]. Quantitatively, effective mass-transfer is governed by a rate coefficient determined indirectly by matching simulated concentrations to chemical tracer data [*Beard and Bassingthwaighte*, 2000a; *Haggerty et al.*, 2004; *Griffioen et al.*, 1998]. That approach is severely limited, since tracer data must exist a priori and must be sampled from spatially representative locations.

[3] Figure 1 displays part of an embedded dendritic network conceptually like the geometry governing relative flow paths when groundwater flows through connected limestone caverns [*Florea and Wicks*, 2001; *Palmer*, 1990] and buried sand-gravel conduits [*Feehley et al.*, 2000; *Harvey and Gorelick*, 2000; *Zheng and Gorelick*, 2003]. As shown in Figure 1, solutes readily migrate through natural conduits while simultaneously diffusing and slowly advecting into adjacent porous media. Similar embedded networks mimic the morphology of vascular-tissue structures. There, advection dominates in multicapillary pathways, [*Vicini et al.*, 1998], and extravascular diffusion governs in tissue [*Beard et al.*, 2003]. Related, but not identical branching structures also occur in certain leaf venation systems [*Roth-Nebelsick et al.*, 2001; *Nelson and Dengler*, 1997], even though xylem networks have an additional mechanical support function, and vessels can taper according to Murray's law [*McCulloh et al.*, 2003].

[4] A common conceptual model underlies transport through conduit-matrix systems where: 1) Preferential fluid migration occurs through complexly connected conduits. 2) Different transport processes dominate in conduits versus matrix owing to disparate permeabilities of each of these domains. 3) Solutes cross the interface between mobile and immobile domains by some combination of molecular diffusion [*LaBolle and Fogg*, 2001] and slow advection [*Zinn and Harvey*, 2003], which are both responsible for rate-limited mass transfer. Where rate-limited mass transfer is significant, permeability contrast across the conduit-matrix interface is typically large and intra-domain variability is relatively small. Therefore, we analyze conduit-matrix binary heterogeneity.

2. Model and Methods

[5] Natural porous media systems involving flow through conductive networks embedded in lower permeability matrix share similar mathematical formulations that quantify transport behavior. In studies of animal tissues, such as brains [*Nagao et al.*, 2001] and hearts [*Beard et al.*, 2003], and natural subsurface flow environments [*Bear*, 1979], identical equations govern even though transport processes are active on different scales. To precisely simulate mass transport, conduit geometry must either be specified based on detailed imaging or synthetically generated using spatial statistical and other structure-imitating construction approaches. Across disciplines, detailed imaging restricted to isolated tissue or small-scale lab rock samples has provided guidance for generating realistic synthetic geometries. Many generation methods are possible [*Stark*, 1991; *Beard and Bassingthwaighte*, 2000b; *Marxen and Henkelman*, 2003].

[6] We implemented a self-avoiding invasion-percolation algorithm [*Stark*, 1991] to represent 3D conductive dendritic structures (Figure 1) and then embedded each complex network in a low-permeability, homogeneous matrix [*Liu et al.*, 2004]. We generated various embedded 3D dendritic networks using the site invasion-percolation algorithm and then pruned the lower four Strahler-order conduit branches [*Strahler*, 1957]. Each generated network is a tree-like

[1]Department of Geological and Environmental Sciences, Stanford University, Stanford, California, USA.
[2]Department of Geological Sciences, University of Alabama, Tuscaloosa, Alabama, USA.

0094-8276/05/2005GL023512$05.00

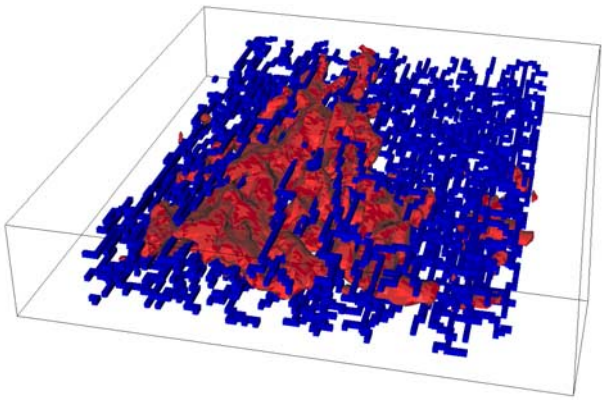

Figure 1. Portion of a 3D dendritic network where conduits occupy 9% of the volume showing an isoconcentration surface. Mass is transported preferentially in conduits. Diffusion and slow advection occur in the matrix. Flow is in the viewing direction.

pattern that is fractal and scale-invariant. Embedded dendritic networks contained 3.8 million cells; 370 cells long, 512 wide, 20 deep. Transport was analyzed in a subregion (370 by 300 by 20 cells). To construct a single dendritic network, a 3D random field of "substrate strength values" [*Stark*, 1991] was generated on a regular cube-cell mesh. Conduits were systematically traced through adjacent cells containing the lowest strength values and constrained to be non-looping. Conduits were initiated at 114 random cells on the downstream plane, which contained 10,240 cells. All conduits have the same cross-sectional area of 10 cm by 10 cm.

[7] To simulate 3D mass transport through dendritic networks embedded in low-permeability homogeneous media, we solved PDEs governing the fluid-potential distribution and changes in solute concentration. The 3D steady-state potential field, Ψ, follows the Laplace equation under a linear gradient-flux relation (Darcy's law), where velocity components are $V_i = -\frac{K}{n_m}\frac{\partial \Psi}{\partial x_i}$ with conductivity K and porosity of the mobile fluid n_m.

[8] Changes in solute concentration due to advection, diffusion, and rate-limited mass transfer are given by [*Zheng and Gorelick*, 2003],

$$n_m \frac{\partial C_m}{\partial t} + n_{im} \frac{\partial C_{im}}{\partial t} = \frac{\partial}{\partial x_i}\left(n_m D^* \frac{\partial C_m}{\partial x_j}\right) - \frac{\partial}{\partial x_i}(n_m V_i C_m) \quad i,j = 1,2,3 \tag{1}$$

$$n_{im} \frac{\partial C_{im}}{\partial t} = \alpha (C_m - C_{im}) \tag{2}$$

for mobile-domain concentration and porosity, C_m and n_m; immobile-domain concentration and porosity, C_{im} and, n_{im}; and molecular diffusion coefficient, D^*. Total porosity is $n = n_m + n_{im}$. Mass-transfer between mobile and immobile domains is governed by α, the mass-transfer coefficient.

[9] When conduits are not sealed and a permeable network is embedded in a less permeable matrix, conduit-matrix mass transfer occurs [*Fogg et al.*, 2000]. Mass transport can be described in detail only if the precise, unique, network-matrix geometry is known. Then 3D concentration changes are determined by (1) in which no distinct immobile porosity is defined, and (2) does not apply. Therefore, advective-diffusive transport simulation involved solving (1) with $C_{im} = 0$ and $n_{im} = 0$.

[10] When exact geometries of embedded networks are unknown, conduit-matrix systems can be modeled as equivalent homogeneous media. This common approach considers bulk equivalent behavior, conduits are not explicitly represented, and there are two domains with diffusive mass transfer occurring between them. In the mobile domain advection dominates diffusion, and in the immobile domain only diffusion occurs. The mobile-immobile domain mass transfer model (1) and (2) yields a gross spatial measure of solute concentration in the matrix, C_{im}, versus concentration in the conduit network, C_m. Advection depends only on the mean fluid velocity, which is simply the total measured volumetric fluid flow divided by the cross-sectional area through which flow occurs. The mass-transfer coefficient, α, is typically estimated through model calibration using experimental tracer concentration data [*Beard and Bassingthwaighte*, 2000a; *Vicini et al.*, 1998], or estimated based on the transport time horizon [*Haggerty et al.*, 2004].

[11] Precise advective-diffusive solute transport in both conduits and matrix was accomplished with a third-order-accurate total variation diminishing (TVD) scheme [*Zheng and Wang*, 1999]. The TVD scheme was used to minimize the effects of numerical dispersion and to ensure that simulations conserved mass. To reduce the local influence of boundary conditions on simulated solute transport, the entire modeled region extended both upstream and downstream of the region containing the embedded network. The conductivity values were assigned as follows: In the embedded network region, the conduit and matrix conductivities were assigned to achieve the specified conductivity contrast for each case studied. In the upstream and downstream buffer zones, outside the embedded-network region, the effective conductivity was assigned as $K_{effective} = \frac{Q}{-\frac{\partial \Psi}{\partial x} A}$, where Q is the discharge through the embedded network region. For most cases examined, the same volumetric flux was maintained even though each had a particular specified conduit-matrix conductivity ratio. That volumetric flux was not maintained for cases in which both conduit and matrix conductivity were varied simultaneously. The solute source was an instantaneous patch occupying 4.7% of the cross section perpendicular to flow in which relative mass was emplaced in proportion to local conductivities. The selection of this patch size was arbitrary but the patch always contained both conduits and matrix. In dimensional terms, each finite-difference 3D cell was 10 cm on a side. Numerical experiments using meshes with finer resolutions of 1/3 and 1/2 cell sizes gave nearly identical results to those using the coarser mesh.

[12] Using simulation [*Zheng and Wang*, 1999], we explored ranges of conduit volume fractions, conduit-matrix conductivity contrasts, and molecular diffusion coefficients. Spatially integrated concentration profiles were computed, accounting in detail for advection and conduit-matrix solute diffusion. Identically integrated concentration profiles were

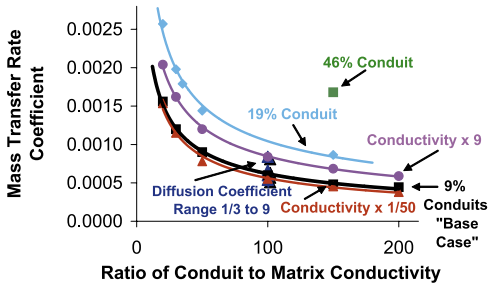

Figure 2. Mass transfer coefficient, α, values (1/day) versus conduit:matrix conductivity ratio. Each α value was estimated using the mass-transfer model to match integrated concentration profiles resulting from solute advection and diffusion in an embedded dendritic network. Parameter variations are relative to the "base case."

obtained by solving (1) and (2) for equivalent homogeneous media. The effective mass-transfer coefficient for each case was estimated by curve-fitting to the tracer concentration profile for advection and diffusion through the exact embedded network.

3. Results

[13] Here we show an alternative to directly obtain effective mass-transfer coefficients. Based on physical arguments involving nondimensional parameter groups, we reasoned that α can be estimated through a relation that does not depend on either matching to conduit-matrix concentration data or knowing the specific geometry of the embedded network. We developed a formula (3) to estimate the mass-transfer coefficient based on these parameter groups. In practice, mass-transfer coefficients can be directly obtained by following two steps: First, generate a representative embedded dendritic network with specified values of conduit volume fraction, f_c, conduit conductivity, $K_{Conduit}$, conduit width, L, matrix conductivity, K_{Matrix}, and diffusion coefficient, $D = n_m D^*$. Second, simulate the fluid potential distribution, Ψ, in the representative system and calculate the mass-transfer coefficient using,

$$\alpha = (\beta)\left[\left(\frac{(D/L)}{\Delta V_{KNR}} + \frac{K_{Matrix}}{K_{Network} - K_{Random}}\right) \times \left(\frac{f_c - \Phi}{\Phi}\right)\right] \qquad (3)$$

where $\Delta V_{KNR} = |V_{KN} - V_{KR}|$, which is the difference between average velocity, V_{KN}, in the entire embedded dendritic network system, and average velocity, V_{KR}, in a completely random heterogeneous conductivity field consisting of the same materials as the dendritic network. $\Phi = \frac{K_{Network} - K_{Matrix}}{K_{Conduit} - K_{Matrix}}$, which can be shown to be the mobile porosity fraction $\frac{n_m}{n}$ when flow is through a simple system of parallel conduits embedded in a less permeable matrix. The value of the constant β, which has the same units as α, was determined to be 0.001875 d^{-1}.

[14] Of importance, we found that ΔV_{KNR} is a meaningful measure of relative connectivity of dendritic networks. It describes the degree to which flow occurs in preferential pathways in structures containing a dendritic network versus flow that occurs through comparable randomized structures with few connected pathways. Fluid velocities V_K in (3) are each based on different homogeneous conductivity fields, K. Velocities are V_{KN} for effective (homogenized) conductivity $K_{Network}$ for a representative conduit network-system, and V_{KR} for effective conductivity K_{Random} when conduit volume is randomly distributed within the low-conductivity matrix. The two effective conductivities, $K_{Network}$ and K_{Random}, were each determined using Darcy's Law written as $K_{Network}$ or $K_{Random} = \frac{Q}{-\frac{\partial \Psi}{\partial x} A}$, where Q is discharge through cross-section A perpendicular to mean flow.

[15] The relation (3) not only yields α but also provides insight into the nature of the mass-transfer processes. Smaller values of effective mass-transfer coefficients correspond to larger conduit-matrix conductivity contrasts, smaller values of diffusion coefficients, greater network connectivities, and lower conduit-volume fractions. Interestingly, we found α does not depend on average flow direction; we obtain the same mass-transfer coefficient values when network flow is reversed, thereby converting conduit tributaries (venous system) into distributaries (arterial system).

[16] We experimented with realizations of embedded networks within a range of conduit densities, conductivity contrasts, and diffusion coefficient values found in natural systems. For example, in networks in cardiac tissue, microvascular volume fraction [*Beard et al.*, 2003] is generally <0.10, and in heterogeneous aquifers [*Feehley et al.*, 2000; *Harvey and Gorelick*, 2000] volume fractions of preferential pathways can be ~0.17 for sediments and higher in channeled limestone. Figure 2 shows the cases investigated. Our "base case" had network realizations with 0.09 conduit volume fraction, 8.64×10^{-6} m^2/d molecular diffusion coefficient, and conduit-matrix conductivity contrasts from 20:1 to 200:1. We also considered a conduit fraction of 0.19 for conduit-matrix contrasts up to 150:1 and a fraction of 0.46 for a contrast of 150:1. The system conductivity was increased 9-fold and reduced to 1/50 for the range of conduit-matrix contrasts. Finally, the diffusion coefficient was decreased to 1/3 and increased 9-fold for a conduit-matrix of 100:1.

[17] Figure 2 relates conduit-matrix conductivity contrasts to effective mass-transfer coefficients. Values of α were estimated based on fitting simulated concentrations using the mass-transfer model ((1) and (2)) to the laterally and vertically integrated tracer concentration profiles generated from detailed advective-diffusive transport through different realizations of embedded networks as described above. Identical estimates of α were obtained by fitting the mass-transfer model results to network tracer concentration profiles at other advective transport distances. This result differs from *Haggerty et al.* [2004], who found that α values increase with increased advective travel. It is possible that for integrated 1D profiles, our finding is caused by the conduit-matrix systems being binary and well dissected by conduits. Increased travel distance does not necessarily result in encountering heterogeneous regimes that serve as "new" immobile domains. Relative-mass histories were obtained at sequential planes perpendicular to mean flow. Across disciplines, this curve-fitting approach has been commonly applied to estimate effective mass-transfer coefficient values. Although Figure 2 exhibits trends, no single relation fits the data.

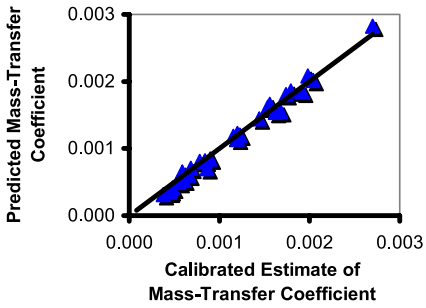

Figure 3. Comparison of "curve fit" calibration estimates to mass-transfer coefficient, α, values (1/day) determined using formula (3). The value of $\beta = 0.001875$ day^{-1} was determined from these data, resulting in $R^2 = 0.986$.

[18] Applying our relation (3), we directly obtained the same effective mass-transfer coefficient values estimated via curve-fitting. In essence, our relation (3) collapses all the points in Figure 2 into a single curve. With $\beta = 0.001875$ d^{-1}, this relation between our α estimates using (3) and those estimated by fitting to the concentration data had an $R^2 > 0.985$ (Figure 3). Note that effective mass-transfer coefficients from calibration are merely estimates, so perfect agreement between those values and α values based on (3) is not likely or desirable.

4. Conclusions

[19] An independent means of estimating conduit-matrix effective mass-transfer coefficients is relevant to different disciplines where mass transfer occurs in structures containing conductive networks embedded in less conductive matrix. One research focus in vascular physiology is determining controls on blood perfusion and oxygen diffusion into tissue. In hydrologic science, there is analogous concern over limitations on solute transfer between preferred pathways and the porous media matrix. Our results suggest that, even though tracer tests are valuable, for permeable media containing a dendritic preferential flow network, mass transfer can be determined without calibrating the effective mass-transfer coefficient by fitting to tracer-test data, if general properties of the network system (i.e., the matrix and conduit conductivities and the cross sectional area and volume fraction of conduits) are available. Uncertainty in these values will of course yield uncertainty in estimated mass-transfer coefficient values.

[20] **Acknowledgments.** This material is based upon work supported by the National Science Foundation under EAR-0003511 and EAR-0003914. Any opinions, findings, conclusions or recommendations do not necessarily reflect the views of the NSF. We thank Paul Hsieh for his 3D visualization software and Daniel Beard and Michael Ronayne for helpful discussions.

References

Barber, P. R., et al. (2003), Semi-automated software for the three-dimensional delineation of complex vascular networks, *J. Microsc.*, *211*, 54.

Bear, J. (1979), *Hydraulics of Groundwater*, McGraw-Hill, New York.

Beard, D. A., and J. B. Bassingthwaighte (2000a), Advection and diffusion of substances in biological tissues with complex vascular networks, *Ann. Biomed. Eng*, *28*, 253.

Beard, D. A., and J. B. Bassingthwaighte (2000b), The fractal nature of myocardial blood flow emerges from a whole-organ model of arterial network, *J. Vascular Res.*, *37*, 282.

Beard, D., K. A. Schenkman, and O. E. Feigl (2003), Myocardial oxygenation in isolated hearts predicted by an anatomically realistic microvascular transport model, *Am. J. Physiol.*, *285*, H1826.

Clemens, T., D. Huckinghaus, R. Lield, and M. Sauter (1999), Simulation of the development of karst aquifers: Role of the epikarst, *Int. J. Earth Sci.*, *88*, 157.

Enquist, B. J. (2002), Universal scaling in tree and vascular plant allometry: Toward a general quantitative theory linking plant form and function from cells to ecosystems, *Tree Physiol.*, *22*, 1045.

Feehley, C. E., C. Zheng, and F. J. Molz (2000), A dual-domain mass transfer approach for modeling solute transport in heterogeneous porous media, application to the MADE site, *Water Resour. Res.*, *36*, 2501.

Florea, L. J., and C. W. Wicks (2001), Solute transport through laboratory-scale karstic aquifers, *J. Cave Karst Stud.*, *68*, 59.

Fogg, G. E., S. F. Carle, and C. Green (2000), Connected network paradigm for the alluvial aquifer system, in *Theory, Modeling, and Field Investigation in Hydrogeology: A Special Volume in Honor of Shlomo P. Neuman's 60th Birthday*, edited by D. Zhang and C. L. Winter, *GSA Spec. Pap.*, *348*, 25.

Griffioen, J. W., D. A. Barry, and J. Y. Parlange (1998), Interpretation of two-region model parameters, *Water Resour. Res.*, *34*, 373.

Haggerty, R., C. F. Harvey, C. Freiherr von Schwerin, and L. C. Meigs (2004), What controls the apparent timescale of solute mass transfer in aquifers and soils? A comparison of experimental results, *Water Resour. Res.*, *40*, W01510, doi:10.1029/2002WR001716.

Harvey, C. F., and S. M. Gorelick (2000), Rate-limited mass transfer or macrodispersion: Which dominates plume evolution at the Macrodispersion Experiment (MADE) site?, *Water Resour. Res.*, *36*, 637.

LaBolle, E. M., and G. E. Fogg (2001), Role of molecular diffusion in contaminant migration and recovery in an alluvial aquifer system, *Transp. Porous Media*, *42*, 155.

Liu, G., C. Zheng, and S. M. Gorelick (2004), Limits of applicability of the advection-dispersion model in aquifers containing connected high-conductivity channels, *Water Resour. Res.*, *40*, W08308, doi:10.1029/2003WR002735.

Marxen, M., and R. M. Henkelman (2003), Branching tree model with fractal vascular resistance explains fractal perfusion heterogeneity, *Am. J. Physiol.*, *284*, H1848.

McCulloh, K. A., J. S. Sperry, and F. R. Adler (2003), Water transport in plants obeys Murray's law, *Nature*, *421*, 939.

Mustafa, S. S., R. J. Richards, and M. D. S. Frame (1999), Microcirculatory basis for nonuniform flow delivery with intravenous nitroprousside, *Anesthesiology*, *91*, 723.

Nagao, M., et al. (2001), Fractal analysis of cerebral blood flow distribution in Alzheimer's disease, *J. Nucl. Med.*, *42*, 1446.

Nelson, T., and N. Dengler (1997), Leaf vascular pattern formation, *Plant Cell*, *9*, 1121.

Palmer, A. N. (1990), Groundwater processes in karst terrains, in *Groundwater Geomorphology*, edited by C. Higgens and D. Coates, *GSA Spec. Pap.*, *252*, 177.

Roth-Nebelsick, A., D. Uhl, V. Mosbrugger, and H. Kerp (2001), Evolution and function of leaf venation architecture: A review, *Ann. Bot.*, *87*, 553.

Stark, C. P. (1991), An invasion percolation model of drainage network evolution, *Nature*, *352*, 423.

Strahler, A. N. (1957), Quantitative analysis of watershed geomorphology, *Eos Trans. AGU*, *38*, 913.

Vicini, P., et al. (1998), Estimation of blood flow heterogeneity in human skeletal muscle using intravascular tracer data, *Ann. Biomed. Eng.*, *26*, 764.

West, G. B., J. H. Brown, and B. J. Enquist (1999), The fourth dimension of life: Fractal geometry and allometric scaling of organisms, *Science*, *284*, 1677.

Zheng, C., and S. M. Gorelick (2003), Analysis of solute transport in flow fields influenced by preferential flow paths at the decimeter scale, *Ground Water*, *41*, 142.

Zheng, C., and P. P. Wang (1999), MT3DMS: Documentation and user's guide, *Contract Rep. SERDP-99–1*, Res. and Dev. Cent., U.S. Army Eng., Vicksburg, Miss.

Zinn, B., and C. F. Harvey (2003), When good statistical models of aquifer heterogeneity go bad: A comparison of flow, dispersion, and mass transfer in connected and multivariate Gaussian hydraulic conductivity fields, *Water Resour. Res.*, *39*(3), 1051, doi:10.1029/2001WR001146.

S. M. Gorelick, Department of Geological and Environmental Sciences, Stanford University, Stanford, CA 94305, USA. (gorelick@pangea.stanford.edu)

G. Liu and C. Zheng, Department of Geological Sciences, University of Alabama, Box 870338, Tuscaloosa, AL 35487, USA.